ISSN 1110-0354
Bull. Nat. Inst. Of Oceanogr. & Fish., A.R.E., 1999. Vol. (25): 1 - 31

LITHOLOGICAL AND HYDROGEOPHYSICAL PARAMETERS OF MARINE SEDIMENTS OF SHARM EL-SHEIKH AREA, RED SEA COAST OF EGYPT

By

SHATA, M. A.* AND HUSSEIN, S. A.

**National Institute of Oceanography and Fisheries, Alexandria, Egypt.*

Key word: Lithology, marine sediments, hydrogeophysical, Sharm El-Sheikh.

ABSTRACT

Fifty six sediment samples, taken from seven boreholes drilled in Sharm El-Sheikh basin, are subjected to laboratory measurements of grain and bulk densities, porosity, cementation factor, electrical resistivity, grain size and elastic modulii.

Some physical models and normograms are constructed to relate the obtained hydrogeophysical parameters to each other. These models characterize the subsurface marine sediments of Sharm El-Sheikh basin and would be reliable for soil test mechanics required in civil engineering.

The cluster delineation of elastic constants indicates that, Sharm El-Sheikh area is affected by a set of faults taking the direction SW-NE, making high cliff at the north of the Sharm basin, while the whole drowned valley is the downside of such tectonism. The neotectonism affects the Sharm through two shallow fracture zones bounding its basin.

From civil engineering point of view, the bedrock favorable for building foundation is going deeper along southwestern direction and is shallower along northeastern direction. Based on the observed fracture pattern taken vertically and laterally along a section passing through the investigated boreholes, the energy released by

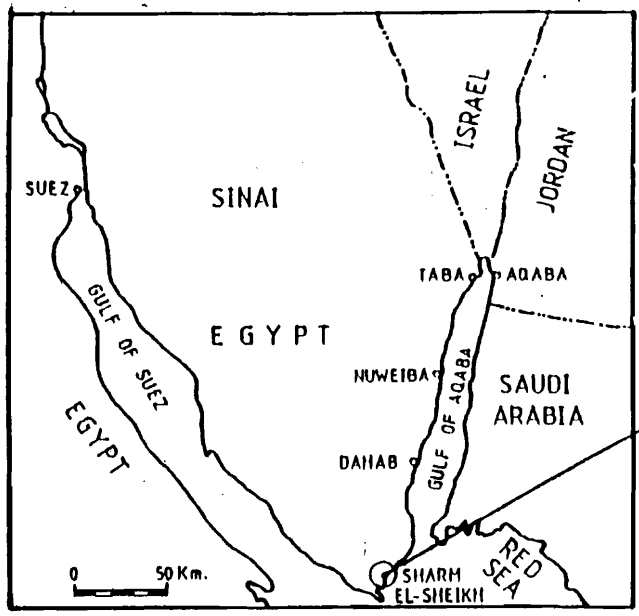

Fig. (1a): Gulf of Aqaba and study area.

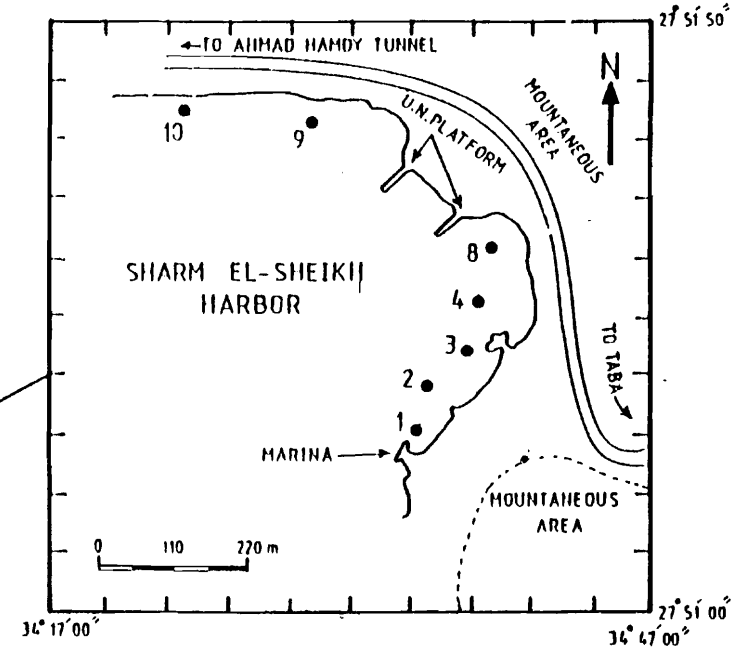

Fig. (1b): Location map of Sharm El-Sheikh (after N.I.O.F.1993).

Morphological and tectonics Setting;

The bottom configuration of the Sharm as revealed from the bathymetric map (Fig.2) measured by NIOF (1993) is in the form of basin like structure sloping downward from north and east toward its central part taking a general form of a drowned fluvial valley. Numerous incised wadies which everywhere showing signs of downcutting dissect the surrounding part of area. Along the beaches of Sharm El-Sheikh, the mountains rise abruptly. The watercourses are streaming from the mountains excavate deep drains with deep sides and steep gradients.

Generally, moderate levels of seismicity and earthquake activities characterize the study area (Parazangi, 1983; and Abd El fattah ***et al***.1997).

The extension of tectonic spreading at the central Red Sea reaches approximately 140 km whereas it had been started from late Miocene (Freund ***et al***., 1970 and McKenzie ***et al***., 1970). Furthermore, the study area obeys "Levant-Aqaba trend" which is a continuation of the Levant active fault that extends along the Gulf of Aqaba and southwest of the Red Sea. It also bisects the clysmic trend at about 27° N and 36° 4' E.

MATERIALS AND METHODS

Fifty- six subsurface sediment samples were taken from seven boreholes drilled in Sharm El-Sheikh bottom (Fig. 1b) which were selected to represent different lithologic units at different depth levels and were subjected to different hydrogeophysical analyses.

Density and Porosity Measurements:

According to a volumetric method described by El-Abd (1985), bulk density σ_b and directly measured porosity ϕ_s of water saturated sediment samples are measured as:

$$\sigma_b = (W_g + V_p \sigma_w)/V_s \quad (1)$$

$$\text{And} \quad \phi_s = (V_s - V_g)/V_s \quad (2)$$

Where:

W_g = Weight of grains in sediment sample .

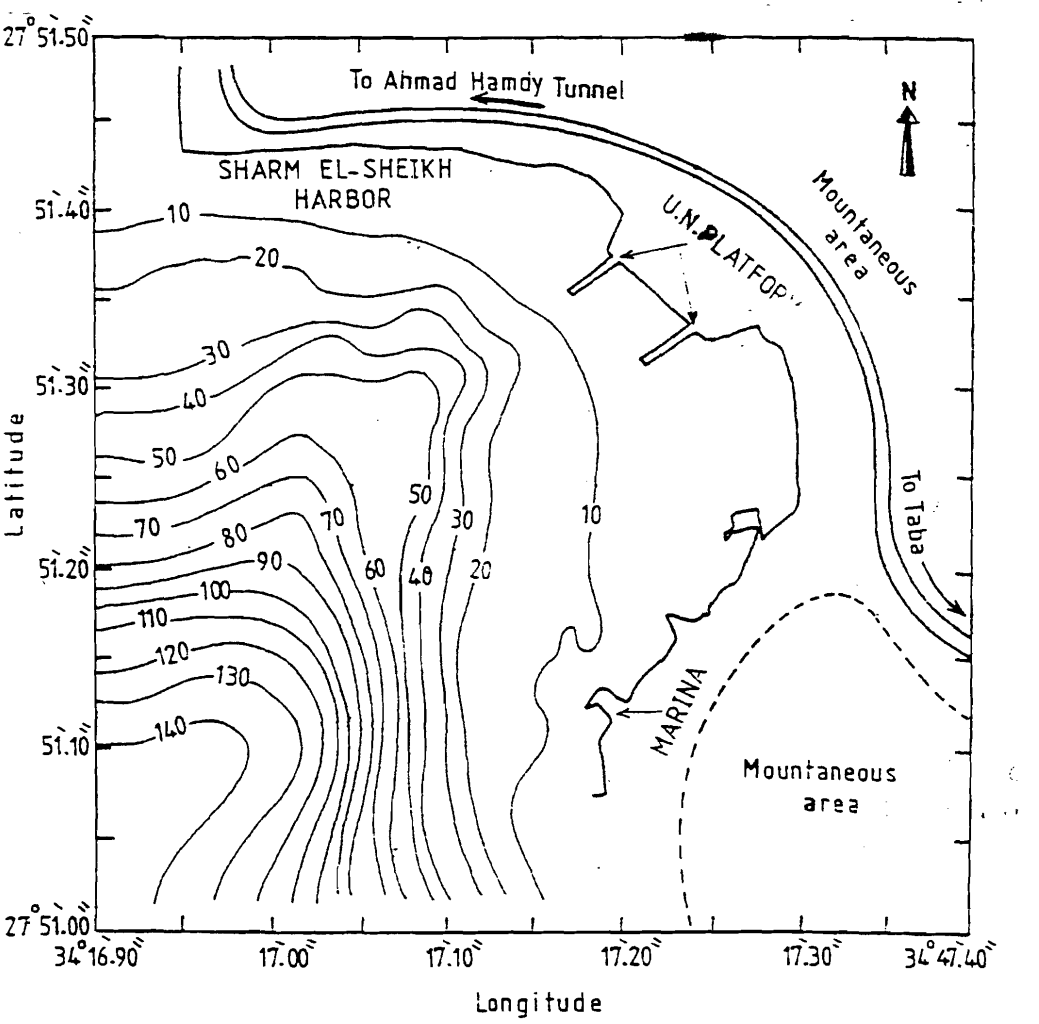

Fig. (2): Bathymetry map of Sharm El-Sheikh (after N.I.O.F. 1993, contour interval 10m.).

V_p = Volume of pores in sediment sample,
V_g = Volume of grains in sediment sample
V_s = Volume of water saturated sample.
The density of solid grains is given by:

$$\sigma_g = W_g/V_g \qquad (3)$$

The error in volumetric measurements was found to be in the order of 4%.

Electrical Resistivity Measurements:

A conductivity meter (Jeanway-4010, Model LF-42) was used for electrical Resistivity measurements. The instrument measures electrical conductance in the range 0.2-110000 micromohos. It has an accuracy of ±2% and is supplied with automatic temperature compensation in the range 0-50° C. The used soil cell is a small rectangular parallelepiped made of Perspex glass of inner dimensions 3.5x3.5x12 cm, with square copper plate electrodes at each end. The Resistivity ρ_s of a regular rectangular parallelepiped sample can be expressed in terms of its electrical conductance C, length L and its cross sectional area A as:

$\rho_s = (1/C) \times (A/L)$
Where, A/L= 1 cm
The accuracy of electrical Resistivity measurements was determined by measuring the Resistivity of a standard KCl-solution (7.4625 gm/1L), which is about 0.78Ω m at 24° C. Accordingly the error in electrical Resistivity measurements was ±4%.

For reefal sediments, where the grain matrix is usually non-conducting, the ratio C_w/C_s is the electrical Resistivity formation factor (F), where C_w and C_s are the conductivity of both seawater and saturated sample. Archie, (1942 &1950) concluded that, for reefal unconsolidated sediment, the variation of (F) with (ϕ_s) is often well defined empirically by the relationship;

$$F = (\phi_s)^{-m} \qquad (4)$$

Where ϕ_s is the measured porosity of the sediments & F is the cementation factor

From the above equation, it is realized that the cementation factor "m" could be quantitatively estimated with a far degree of precision after calculation of ϕ_s & F.

Elastic modulii and sound waves Estimation:

Using the graphical relationships between porosity ϕ and each of young's **E** and shear μ modulii, compressional V_p and shear V_s seismic wave velocities which measured in some of offshore basins in Gulf of Suez (Ibrahim, 1993), it could estimate the different values of elastic modulii of the marine sediments (Figs.3a-e). In fact, these results were obtained as being for in situ sediments after slight normalization of the laboratory measurements i.e. $\phi_{situ}=\sqrt[n]{\pi L\ \phi_n}$

Where n varies from 100% to 70% of the laboratory measurement and L is the length of the measured samples.

The porosity/ elastic modulii and seismic velocity relations are previously suggested by (Eliot & Wiley, 1975; Gregory, 1976 Tathan and Staffa, 1976 and Winkler & Nur, 1982)

Statistical Analysis:

According to variety of descriptive statistical procedures calculations of average, medium, variance, standard deviations, minimum, maximum and range as well as formation of histograms are allowed.

Summary of data distribution has been represented in a table of frequencies and cumulative frequencies after grouping the data into a selected number of class intervals bounded between upper and lower limits of the petrophysical data of the borehole samples. Geometric mean is used to average index numbers of the petrophysical data expressed as ratios or percentages, while the weighted average is applied on non-equally important data through appropriate weightily factors. The applied statistical procedure used in this work are introduced by (Box and Jenkins, 1976), (Cox and Lewis, 1966) and (Morrison, 1967). The sum of products of the variables and the correlation coefficient in addition to the standard deviations can be calculated. Regression analysis is used to relate one dependent variable of the present set of parameters to one independent variable (in simple regression) or many independent variables (in multiregression), by minimizing the sum of the squares of the residuals for the fitted line. The polynomial expression of the regression analysis could be expressed in a form of integer powers of the independent variables to have curvilinear regression analysis, (Draper and Smith, 1966) and (Polhemus, 1982).

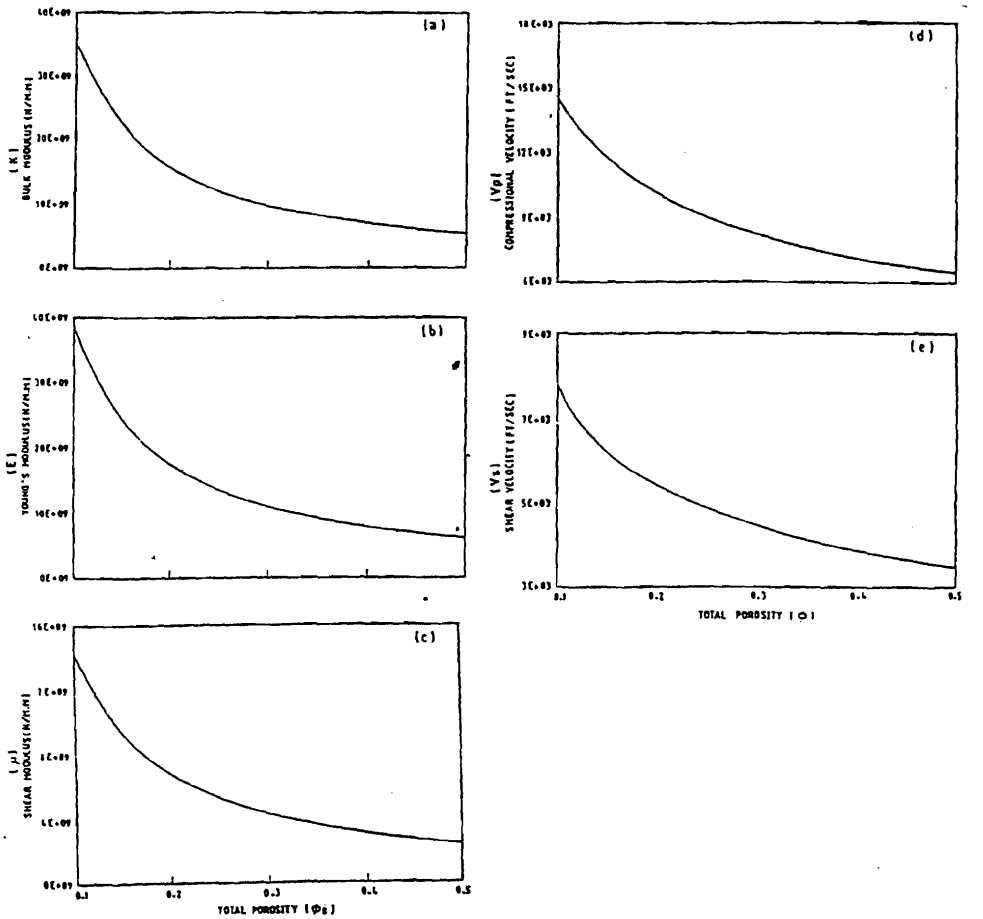

Fig. (3a-e): Graphical relationships between porosity ϕ and a; bulk (k) b; Young's (E) c; Shear (μ) modulii d; compressional (V_p) - and shear (V_s) – Seismic velocities (after Ibrahim, 1993).

Least-squares regression analysis is used to estimate the models that are always associated with calculation of variance (Tatsuoka, 1971 and Tukey, 1977). The last procedure was applied in constructing models of large number of independent variables. If we consider the polynomial regression model equation in the form

$$Y = \beta_0 + \beta_1 X_1 + \beta_2 X_2 + \ldots \beta_m X_m + \in \quad (5)$$

Where Y is the dependent variables and X_1, $X_2 \ldots X_m$ are the independent variables, $\in$ is the residual error between the modeled and the observed **Y's** and β **'s** are the coefficients to be obtained by least square solution of linear equation by solving a set of normal equations as:

$$[\Sigma X].[\beta] = [\Sigma Y] \quad , \quad \beta = [\Sigma X]^{-1}.[\Sigma Y] \quad (6)$$

RESULTS AND DISCUSSIONS

Lithological characteristics:

According to Awad *et.al.* (1998), the paleoshoreline in the area of investigation is at depths of -18.8, -18.0, -20.0 and -16 m in the boreholes of the eastern flank and at -9.6, -6.0 and -9.3 m in boreholes of the northern flank as indicated from dominant medium to fine sand as well as intertidal foramineferal tests and evaporitic minerals.

The mineralogical analysis reveals the presence of reefal communities occupying the upper parts of the subbottom sediments that are subjected to intensive evaporation favorable for carbonate diagensis at some depth levels. Admixtures of carbonate and noncarbonate components depending on the amounts of terrestrial contributions underlaid the upper succession, whereas the silisiclastic minerals are confined to the lower parts of the subbottom sediments derived mainly from the granitic cliffs.

The results of grain size and mineralogical analyses, as well as, field standard penetration test (SPT) have been compiled and interpreted to get a tentative lithologic section (Fig.4) along the seven boreholes. Inspection of this

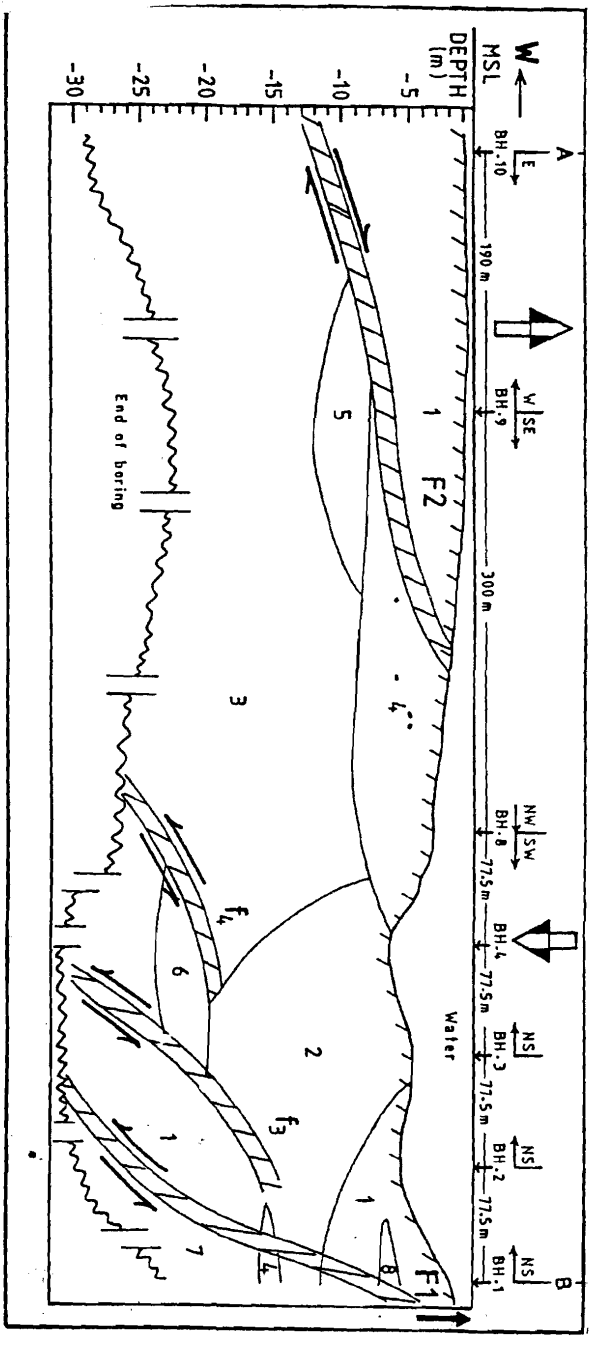

Fig. (4): Compiled lithologic section along the sector AB in Sharm El-Sheikh Harbor

section shows that it includes 8 different lithologic features, which is described and summarized in table 1.

The existence of some lens structures (layer No.4, 5, 6 and 8) indicates the paleoenvironmental conditions, of fluviomarine origin. The compiled section shows the effect of the two shallow fractures F_1 & F_2 together with the small features of deeper ones f3 and f4. Also the carbonate mineral contents have been used as a possible indicator for Holocene sea level variations (Awad *et. al.*, 1998)

Petrophysical parameters:

A comprehensive pictures of subsurface settings, concerning number of blows (N) which reflect the hardness or compaction of sediments; grain density (σ_g); bulk density (σ_b); measuring porosity (ϕ_s); electrical Resistivity, formation factor (F) and cementation factor (m) are presented in table (2). The obtained values of the elastic modulii (shear modulus μ, bulk modulus K, Young's modulus E and sound velocities (shear wave velocity V_s and comperessional wave velocity V_p) are shown in table (3), whereas the elastic modulii ranges are summarized in table (4).

Petrophysical properties of Sharm El-Sheikh subbottom sediments are mainly related to the degree of compaction or hardness (i.e., number of blows ,N obtained from the standard penetration test SPT), grain and bulk densities (σ_g & σ_b), cementation factor m, electrical Resistivity ϕ formation factor F and the measured porosity ϕ_s. Vertical and lateral variations of the compiled values of the above said parameters with depth are illustrated in Fig. (5a & 5b). Also all of these compiled petrophysical parameters for the seven wells are plotted with depth to form a sort of clusters plot, as shown in Fig. (6).

Inspection of Fig. (6) shows that, subbottom sediments in Sharm El-Sheikh could be sorted in 7 layers, whereas the gaps between these layers represent transitional zones at which the petrophysical parameters changed. The most recent and shallowest layer (1) is at depth range from 1-2 m below mean sea level. The oldest and deepest layer (7) is at depth range from 25.5-29.5 m. The intermediate layers (2,3,4,5 and 6) are at depth ranges; 3-7m, 9-12.5m, 13.5-16m, 19.5-21.25m and 22.5-24m respectively. These layers are characterized by continuous deposition that may be intermittent by non-depositional periods.

Table (1): Compiled Lithologic description of subsurface layers in Sharm El-Sheikh, Red Sea.

Layer.	Lithology
1	Well rounded granite cuttings with pink to brown color, shell fragments of gastropods with white, yellowish brown to brown colour, patches of coral reef and foramineferal tests of different sizes. Medium to fine sand, traces of (dolomite, siderite, ankerite and heavy mineral). Clastic/ non-clastic ratio 2:1, N 25
2	Mainly pure carbonate sediments, Coral reef fragments of gravel size. Little amount of Q_Z, granite cuttings, and shell fragments of yellowish to white colour, poorly to medium sorted. Clastic/ non-clastic ratio 0.0: 1, N 30:40
3	Mainly Nubian Sandstone deposits, coarse to very fine sand sized, brownish yellow to yellow colour. Traces of feldspars, anhydrite, ankerite, shell fragments, few amount of granite grains, heavy minerals, foramineferal tests (intertidal zone). Clastic/ non-clastic ratio 1.0: 0.0 N 125:150.
4	Coarse fragments of limestone, shells of gravel size of gastropods, bivalves, foramineferal tests, coral reef fragments, dark colour due to heavy minerals, poorly sorted with medium sand size, little amount of fine sand of greywish white colour with pink granite, it is considered as the lower boundary of the carbonate layer. Clastic/ non-clastic ratio 1:2 N 20:25
5	Lens structure of reddish brown Nubian sandstone deposited as Sabkha sediments (13.6% clay + 2.0% anhydrite) mainly clastic sediments, poorly sorted with medium sand sized, traces of carbonate minerals (dolomite, ankerite). Clastic/ non-clastic ratio 1: 0.0, N 150
6	Lens structure of fine sand poorly sorted clastic minerals, brownish silt fraction, traces of L.S. of black colour as coarse fraction, clay as kaolinite 13.3%. Clastic/ non-clastic ratio 1.0: 0.0 N, 150:175.
7	Composed mainly of granite cuttings of very coarse sand sized poorly to moderately sort with reddish brown to pink colour with traces of coral reef fragments. Clastic/ non-clastic ratio 1.0: 0, N 40:50.
8	Small lens composed of coral reef fragments, broken shell fragments, granite cuttings, clay 8.5%, poorly sorted. N 50:60.

N = Number of blows per each 6 inches (from SPT).

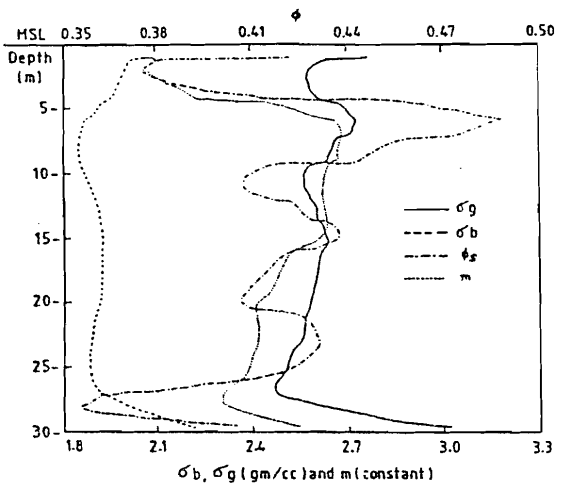

Fig. (5a): Compiled logs showing the variations of σ_g (grain density); σ_b (bulk density); (ϕ_s) porosity and cementation factor (m) with depth in Sharm El-Sheikh subbottom sediments.

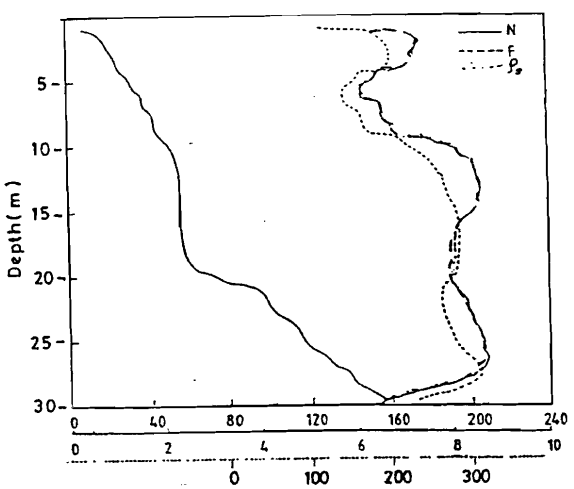

Fig.(5b): Compiled logs showing the variations of ρ_s (electrical Resistivity);F (formation factor and number of blows (N) with depth in Sharm El-Sheikh subbottom sediments.

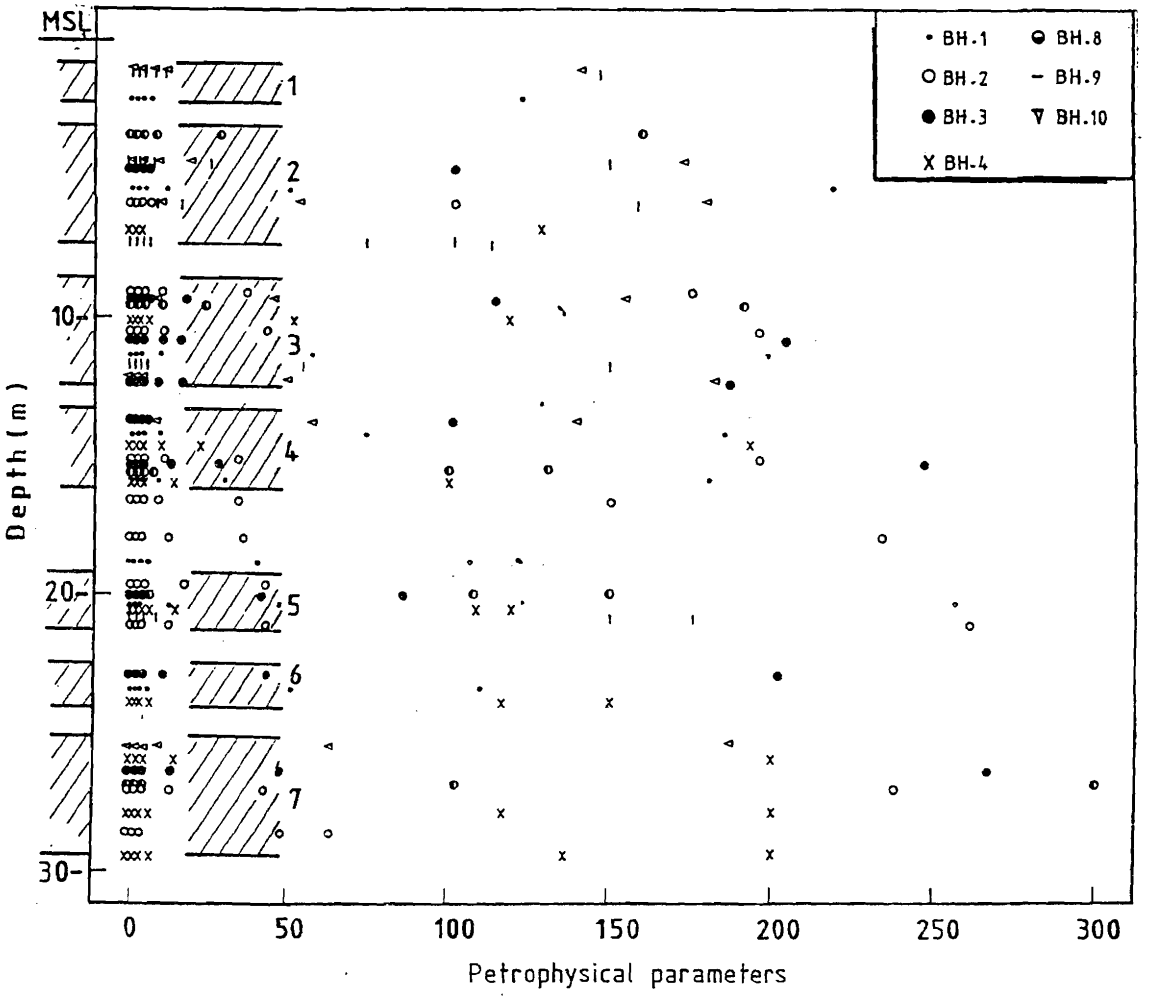

Fig. (6): Subbottom layering in Sharm El-Skeikh as revealed from the compiled logs of petrophysical parameters.

The compiled petrophysical data for the whole depth and the number of blows (N) ranges of the seven wells were modeled to be in the form of 8^{th} order continuous polynomial in the form of;

$$Y_p = \sum_{i=0}^{8} a^{pi} d^i \qquad \ldots\ldots\ldots\ldots\ldots\ldots \quad 7$$

Where; "Y_p" is the parametric variable of certain petrophysical property "p" and a^{pi} is the p th constant of i order, d^i is the depth to the I th power. Figs. (5a & 5b) present the variations of the compiled parametric variables (σ_g, σ_b, ϕ_s and **m**), (**N**, **F** and ρ_s) respectively. Inspection of these figures shows that;

σ_g, and **m**, curves (Fig.6) reveals good criteria of layers classification, into seven layers according to the boundaries defined by their inflection points located between the local highs and lows indicated in curves of Fig.(5a & 5b). This may confirm the above results obtained from the compiled observed logging data. However, σ_b does not show great variation except within the depth ranges from (1-8) m and (26-30) m. Figures (4a &4 b and5) are favorable for the determination of soil test mechanical parameters necessary for civil, coastal and marine construction in the study area.

Physical models of the study area:

Multiple regression analysis has been carried out to get an optimum relation between porosity "ϕ_s" and other petrophysical parameters of the sediments. The analysis shows that there is a slight deviation from the well logging measured porosity. The mathematical models of the porosity "ϕ_s" are obtained firstly for each of the seven wells, in terms of densities (σ_g & σ_b) with depth (D):

The general model equation for the whole subsurface marine sediments of the Sharm is then obtained:

$$\phi_s = 4.17571 \times 10^{-4} (D) + 0.3792937 (\sigma_g) - 0.6032428 (\sigma_b) + 0.591885 \qquad 8$$

The deviations of "ϕ", as well as, the number of blows along the depths of the seven boreholes are shown in figures (7a & 7b) which must be considered in making the correction of "ϕ" (if any) at and near each location of the seven boreholes, in favor of civil engineering marine constructions.

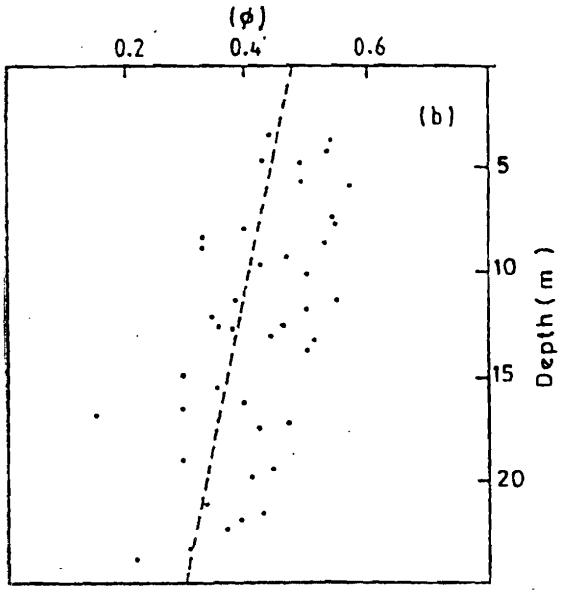

Fig. (7a): Porosity (ϕ_s/ Depth trend of subbottom marine sediments of Sharm El-Sheikh basin.

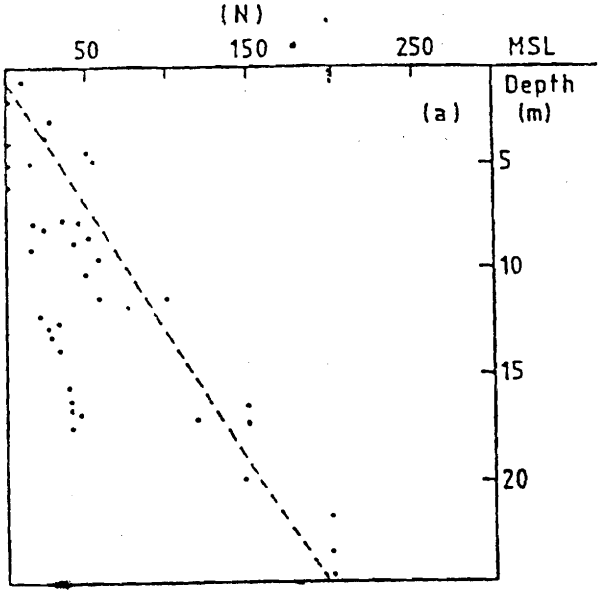

Fig. (7b): Number of blows / Depth trend of subbottom marine sediments of Sharm El-Sheikh basin.

Also, the mathematical models representing the relations between porosity and both of expected number of blows "N" and depth from sea level, are represented by the following straight line fitting equations

N = 5.591 (D) - 15.823
9

ϕ % = - 0.0078 (D) + 0.5447
10

The graphical trends of these two equations are shown in figures (7a & b).

Normograms of marine subsurface sediments in study area:

As far as marine sediments are concerned, new normograms were constructed relating the porosity "ϕ_s" with each of: Bulk density "σ_b" and grain density "σ_g" as shown in Fig. (8a&8b), which consists of seven categories of "σ_g" ranges. Another normograms relating porosity "ϕ**i**" to electrical Resistivity, formation factor "**F**" and cementation factor "**m**" are shown in Fig. (9a-c) which consists of eight categories of "**m**". Moreover, the mathematical matrix model equation of the first set of normograms is as following:

$$[(\sigma b)i] \equiv \begin{bmatrix} 2.2795 & -1.573 \\ 2.445 & -1.573 \\ 2.5582 & -1.573 \\ 2.6474 & -1.573 \\ 2.6841 & -1.573 \\ 2.7228 & -1.573 \\ 2.8910 & -1.573 \end{bmatrix} \times \begin{bmatrix} 1 \\ \phi i \end{bmatrix}$$

Where i is assigned for the category of " σ_g" which ranges between 2.3 and 2.8 gm/cc.

i = 1		**σ_g < 2.35**
i = 2	**2.35**	**σ_g < 2.5**
i = 3	**2.50**	**σ_g < 2.57**
i = 4	**2.75**	**σ_g < 2.70**

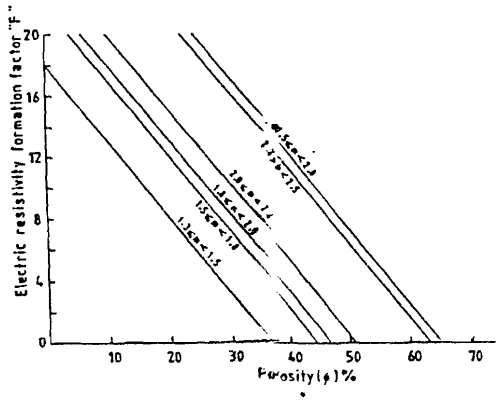

Fig. (8a): Normogram of electrical Resistivity / porosity at constant values o f cementation factor (m) for subbottom sediments of Sharm El-Sheikh basin.

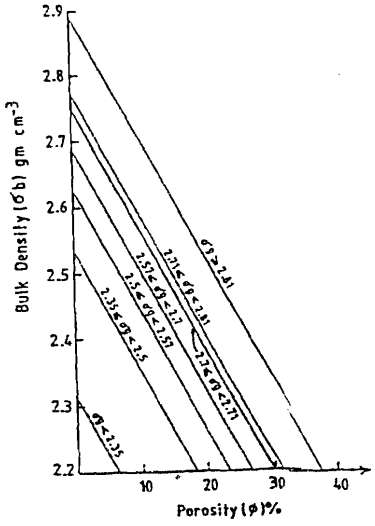

Fig. (8b): Normogram of bulk density / porosity at constant values of grain density for subbottom sediments of Sharm El-Sheikh basin.

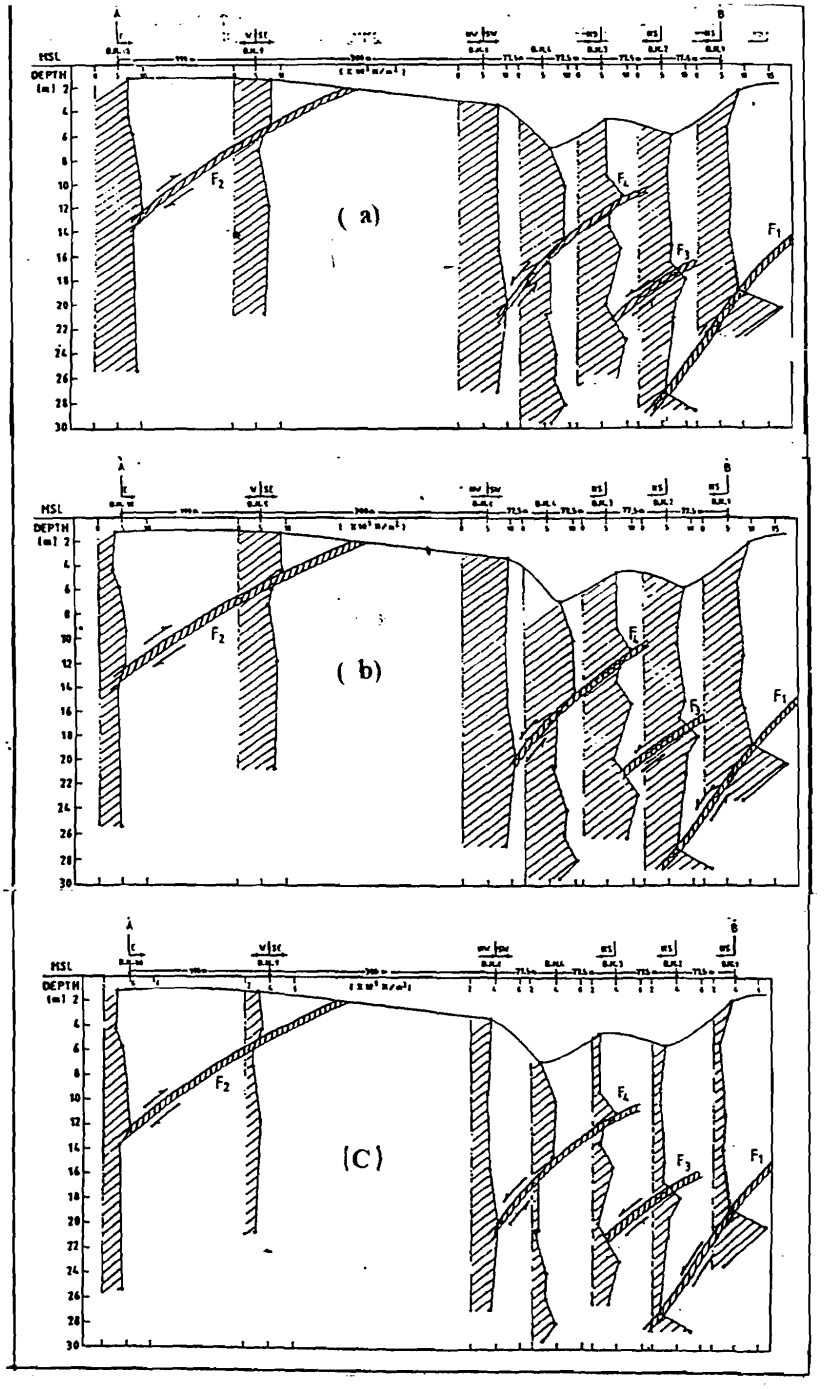

Fig. (9): Vertical variations of a; Young's (E), b; Bulk (K) and c; Shear (μ) modulii in the seven boreholes with faults structure along the sector AB in subbottom sediments of Sharm El-Sheikh basin.

i = 5	**2.70**	**σ_g < 2.71**
i = 6	**2.71**	**σ_g < 2.81**
i = 7		**σ_g 2.81**

While the mathematical matrix model equation of the second set of normogram is as following;

$$[(F)i] \equiv \begin{bmatrix} 18 & -94.1 \\ 22 & -94.1 \\ 23 & -94.1 \\ 25 & -94.1 \\ 31 & -94.1 \\ 32 & -94.1 \\ 34 & -94.1 \\ 40 & -94.1 \end{bmatrix} \times \begin{bmatrix} 1 \\ \phi i \end{bmatrix}$$

Where i is assigned for the category of "m" as following

i = 1	**1.3**	**m 1.5**
i = 2	**1.5**	**m < 1.8**
i = 3	**1.8**	**m < 2.0**
i = 4	**2.0**	**m < 2.2**
i = 5	**2.2**	**m < 2.5**
i = 6	**2.5**	**m < 2.8**
i = 7	**2.8**	**m < 3.0**
i = 8		**m 3.0**

Where i is the category of σ_g, which ranges between 2.3 and 2.8 gm/cc. The general average model equation of this normograms is computed as:

$$\sigma_b = 2.6\text{-}1.57 \text{ "}\phi i\text{"} \qquad 13$$

Where "ϕ_i" is in decimal fraction. This means that, the average value of grain density of sediments in subbottom of the Sharm is about 2.6-gm/cc i.e. mainly due to the carbonate sediments El-Abd (1985).

Another normograms (Fig.8b) relates "ϕi" to electrical Resistivity, formation factor (F) and cementation factor (m) is constructed. The mathematical model in matrix form of this normograms is:

$$F = 25 - 0.5\,\phi_s \qquad 14$$

Where ϕs is in %

Or :

$$F = \phi_s^{-2.1} \qquad 15$$

These sets of normograms together with the "N" chart are helpful in design the bearing capacity of heavy marine civil engineering buildings in Sharm-El-Sheikh basin

Elastic modulii;

Analysis of elastic constant variations of Sharm El-Sheikh subbottom sediments as shown in figures (9&10), both laterally and vertically, indicate that:

(a) The cluster delineation of the high and low values of these constants reveals some faults that affect the area from the south western (deep effect) to the north eastern directions (shallow effect). These sets of faults are making up and down thrown sides. Accordingly, the northern part of the basin is characterized by a high cliff while the whole drowned valley is characterized by a down side of tectonism;

(b) The minimum and maximum values of (μ, K, E, V_s and V_p) table (3) show that, the lateral variations of these constants are almost uniform and of low dispersion within the space domain from BH. 10 to BH.8, as indicated by irregular curves Figs (10 & 11). The part of the profile from BH. 8 to BH. 1 is non-uniform and of wide dispersion as indicated by smooth curves. This may indicate the effect of recent tectonism, which affect the area through two fracture zones F_1 & F_2 bounding the Sharm basin. The axis of the basin is well defined near the location of BH.9, as seen in the bathymetric map (Fig.2).

Table (2): Measured petrophysical parameters of subbottom sediments in Sharm El-Sheikh, Red Sea.

B.No.	Depth. SL.	No. Blow	σ_g	σ_b	(ϕ_s)	C	(ρ_s)	F	m
1-1	-2.10	20	2.609	2.083	0.3611	0.0108	123.457	6.296	1.806
1-3	-5.32	51	2.744	1.815	0.5327	0.0061	218.579	11.148	3.828
1-7	-11.37	58	2.533	1.817	0.4666	0.0067	199.005	9.552	2.961
1-9	-14.20	75	2.834	1.917	0.5000	0.0072	185.185	8.611	3.106
1-10	-15.82	29	2.571	1.880	0.4400	0.0074	180.180	8.379	2.589
1-12	-18.81	39	2.611	2.038	0.3558	0.0125	106.667	4.960	1.550
1-13	-20.32	47	1.882	1.750	0.1500	0.0052	256.460	11.923	1.306
1-15	-23.42	51	2.500	1.927	0.4483	0.0121	110.193	5.124	2.037
2-1	-5.90	20	2.808	2.033	0.4290	0.0130	102.546	5.462	2.006
2-3	-9.12	36	2.750	1.795	0.5450	0.0080	175.439	9.342	3.681
2-4	-10.52	43	2.746	1.819	0.5310	0.0070	196.078	10.000	3.638
2-7	-15.12	33	2.477	1.795	0.4620	0.0070	196.078	10.000	2.982
2-8	-16.62	33	3.002	2.001	0.5000	0.0080	156.863	8.118	3.021
2-9	-17.97	35	2.508	2.056	0.3000	0.0060	233.918	11.930	2.059
2-10	-19.62	42	2.737	2.042	0.4000	0.0040	333.333	16.525	3.061
2-11	-21.12	42	2.861	2.071	0.4240	0.0050	261.438	11.765	2.873
2-14	-27.10	42	2.888	1.850	0.5500	0.0060	238.095	12.143	4.176
2-15	-28.62	48	2.891	2.471	0.2220	0.0010	156.860	8.118	3.021
3-1	-4.62	20	2.714	1.785	0.5417	0.0130	102.564	4.815	2.564
3-4	-9.34	17	2.737	1.785	0.5484	0.0116	114.943	5.397	2.806
3-5	-10.84	15	2.214	1.784	0.3330	0.0065	205.128	9.631	2.060
3-6	-12.34	16	2.666	1.810	0.5000	0.0071	187.793	7.831	2.970
3-7	-13.69	100	2.771	1.833	0.5500	0.0131	101.781	5.076	2.717
3-8	-15.24	27	2.692	1.797	0.3585	0.0054	246.914	12.314	2.448
3-11	-19.91	41	2.378	2.085	0.6038	0.0155	86.022	4.071	2.713
3-13	-22.84	43	2.665	1.546	0.3000	0.0066	202.020	9.606	1.879
3-15	-26.34	48	2.473	2.166	0.3929	0.0050	266.666	12.680	2.719
4-1	-6.95	20	2.872	1.287	0.4915	0.0103	129.450	1.319	0.3390
4-3	-10.17	52	2.305	1.952	0.3330	0.0112	119.048	5.527	1.5550
4-6	-14.67	21	2.285	1.870	0.3479	0.0069	193.237	9.058	2.0870
4-7	-16.02	100	2.656	1.838	0.5161	0.0010	187.790	7.831	2.9700
4-10	-20.56	120	2.749	1.801	0.5625	0.0010	187.790	7.831	2.970
4-10	-20.60	120	2.384	1.765	0.5909	0.0124	107.527	5.089	3.0930
4-12	-23.99	150	2.608	1.566	0.4118	0.0114	116.959	5.535	1.9290

4-13	-25.98	200	2.550	1.946	0.4286	0.0010	116.959	5.535	1.9290
4-14	-27.98	200	2.571	1.886	0.3115	0.0114	116.959	5.535	1.4670
4-15	-29.48	200	2.865	2.081	0.4701	0.0098	136.054	6.378	2.4550
8-1	-3.40	28	2.521	1.988	0.4000	0.0083	160.643	7.675	2.0520
8-5	-9.62	23	2.574	1.957	0.4000	0.0068	196.078	9.368	2.4420
8-9	-15.48	100	2.596	1.944	0.4000	0.0102	130.719	6.177	1.856
8-12	-19.95	150	2.639	1.998	0.3000	0.0124	107.527	5.790	1.459
8-17	-26.90	300	2.623	2.148	0.4000	0.0130	102.564	5.300	1.682
9-1	-1.20	10	2.714	2.040	0.4015	0.0091	146.520	7.000	2.103
9-3	-4.40	24	2.568	2.026	0.3728	0.0089	149.810	7.000	1.967
9-4	-5.90	15	2.604	1.983	0.4902	0.0084	158.730	7.000	2.804
9-5	-7.30	75	2.817	1.818	0.5686	0.0131	101.780	5.000	2.891
9-5	-7.40	75	2.321	1.784	0.5714	0.0118	112.990	5.000	2.879
9-8	-11.80	150	2.742	1.566	0.4301	0.0010	146.520	7.000	2.130
9-13	-20.80	150	2.884	1.992	0.4722	0.0076	175.440	8.000	2.733
10-1	-1.10	11	2.704	1.994	0.4166	0.0094	141.844	6.660	2.165
10-3	-4.33	18	2.580	1.881	0.4424	0.0077	173.160	8.130	2.569
10-4	-5.83	54	2.663	2.033	0.3786	0.0074	180.180	8.460	2.599
10-7	-9.33	45	2.650	2.138	0.0310	0.0086	155.039	7.279	1.696
10-9	-12.25	50	2.533	2.071	0.3014	0.0073	182.648	8.575	1.792
10-10	-13.73	58	2.644	2.012	0.3846	0.0095	140.350	6.590	1.973
10-18	-25.42	63	2.583	2.049	0.3375	0.0071	187.793	8.817	2.004

σ_g = Grain density (gm/cc) **(ρ_s) = Electrical Resistivity (ohm.m)**

σ_b = Bulk density (gm/cc) **F = Electrical Resistivity formation factor**

(ϕ_s)= Porosity (in fraction) **m = Cementation factor**

C= Conductivity (moh.m)

(c) From civil engineering point of view, the bedrock favorable for foundation of buildings is deeper as we go along southwestern direction and is shallower as we go along northeastern direction (i.e. along Aqaba trend).

(d) Seismologically and Based on the observed fracture pattern taken vertically and laterally along a section passing through the investigated boreholes, the energy released by earthquakes is always expected to migrate from the deeper origin (in the southwestern part)

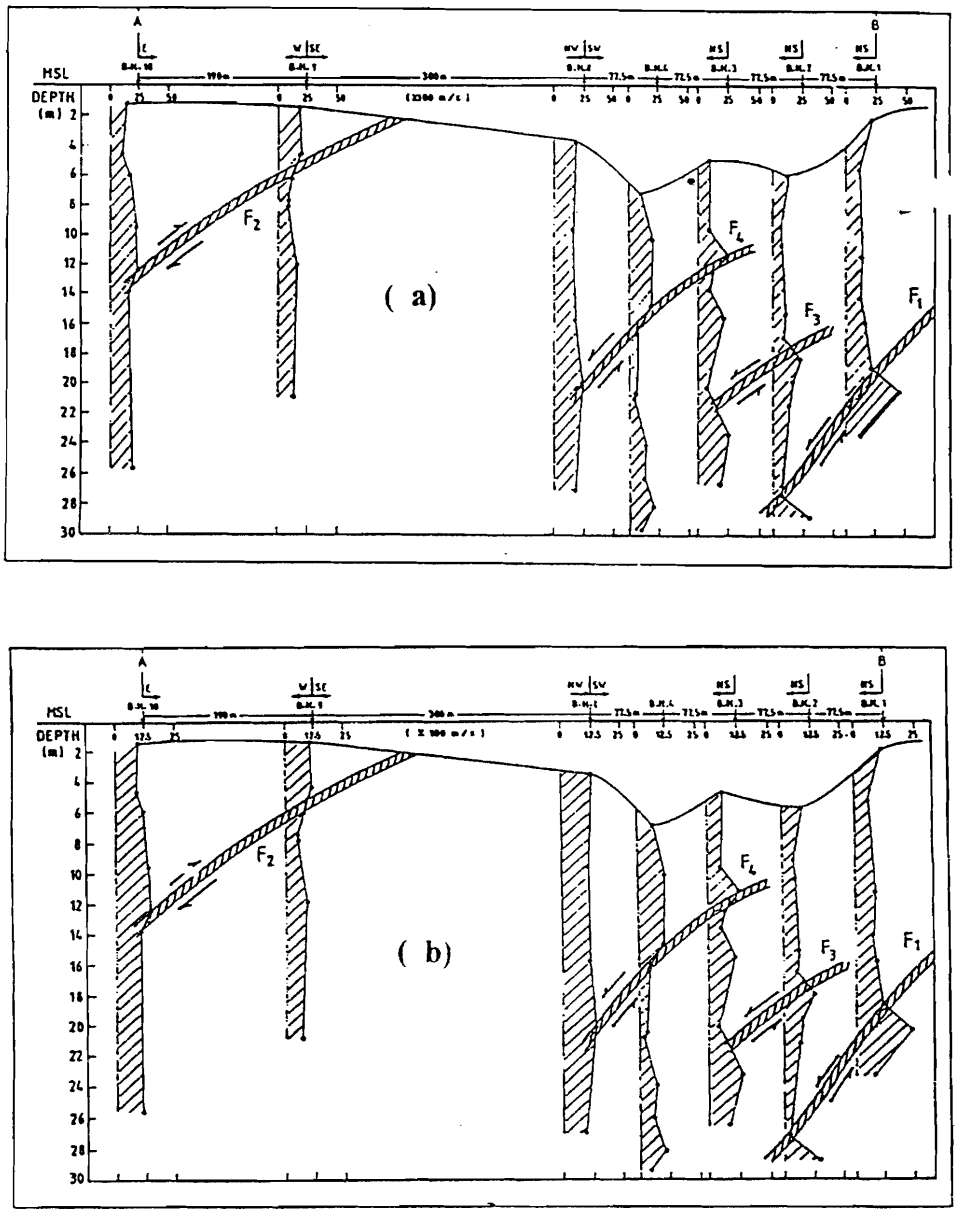

Fig. (10): Vertical variations of a; compressional wave (Vp) and b; shear wave velocities of sound in the seven boreholes with faults structure along the sector AB in subbbottom sediments of Sharm El-Sheikh basin.

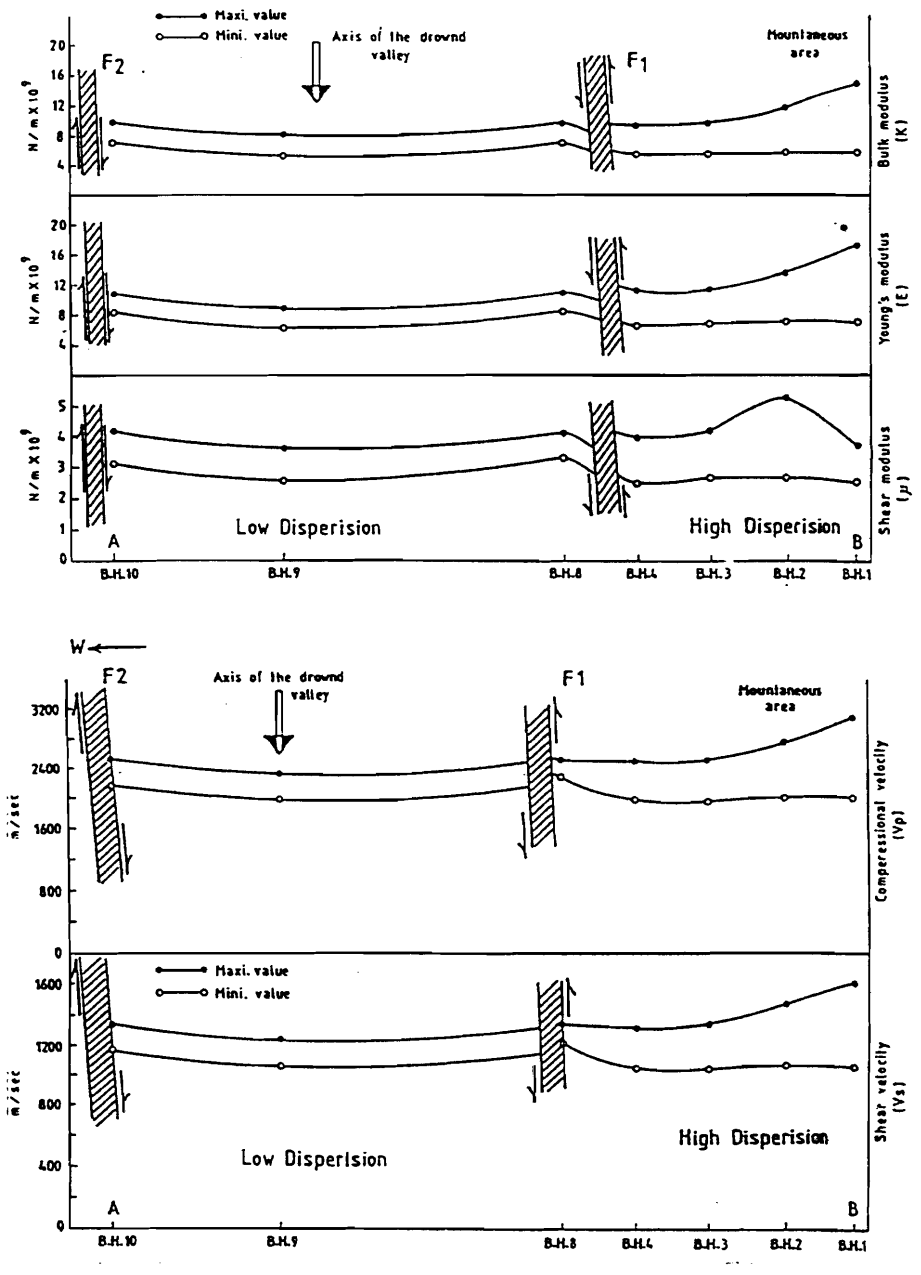

Fig. (11): Structural framework Sharm El-Sheikh basin as predicted from the variations of elastic moulii and seismic wave velocities along the sector AB.

Table (3): Indirectly measured values of elastic modulii of subsurface sediments in Sharm El-Sheikh, Red Sea.

Borehole No.	Depth (BPSL) "m"	(μ) N/m^2	(K) N/m^2	(E) N/m^2	(V_s) m/sec	V_p m/sec
		x 10^9	X 10^9	x 10^9		
1-1	2.10	3.63	8.31	9.58	1258	2367
1-3	5.33	2.61	5.94	6.85	1086	2038
1-7	11.33	2.95	6.65	7.79	1145	2155
1-9	14.20	2.78	6.20	7.32	1113	2095
1-10	15.83	3.07	6.95	8.15	1171	2196
1-12	18.82	3.46	8.35	9.65	1262	2375
1-13	20.33	6.63	15.26	17.27	1628	3099
1-15	23.43	3.07	6.91	8.11	1166	2190
2-1	5.90	3.16	7.09	8.38	1178	2220
2-3	9.13	2.60	5.77	6.73	1079	2018
2-4	10.53	2.61	5.91	6.92	1086	2038
2-7	15.13	2.93	6.69	7.83	1150	2166
2-8	16.63	2.78	6.20	7.32	1113	2095
2-9	17.98	4.17	9.57	11.07	1341	2523
2-10	19.63	3.30	7.65	8.82	1216	2281
2-11	21.13	3.20	7.17	8.39	1187	2234
2-14	27.10	2.60	5.66	6.69	1072	2011
2-15	63	5.16	1.88	13.65	1473	2771
3-1	4.62	2.61	5.36	6.85	1081	2022
3-4	9.35	2.60	5.36	6.77	1079	2018
3-5	10.85	3.86	8.78	9.58	1295	2436
3-6	12.35	2.78	6.20	7.36	1113	2095
3-7	13.70	2.60	5.66	6.69	1072	2011
3-8	15.25	3.62	8.35	9.70	1262	2376
3-11	19.95	2.43	5.27	6.27	1047	1972
3-13	22.85	4.17	9.57	11.14	1341	2523

3-15	26.35	3.37	7.66	8.93	1221	2295
4-1	7.00	2.83	6.37	7.39	1122	2110
4-3	10.18	3.86	8.78	10.17	1295	2436
4-6	14.68	3.70	8.50	10.12	1276	2395
4-7	16.03	2.71	6.05	7.16	1101	2066
4-10.1	20.57	2.58	5.99	6.65	1066	2000
4-10.2	20.60	2.48	5.30	6.40	1052	1985
4-12	24.00	3.28	7.46	8.66	1201	2256
4-13	26.00	3.16	7.17	8.47	1178	2220
4-14	28.00	4.03	9.28	10.99	1322	2487
4-15	29.49	2.95	6.50	7.79	1142	2149
8-1	3.40	3.56	8.00	9.41	1247	2345
8-5	9.63	3.30	7.65	8.87	1216	2281
8-9	15.48	3.53	8.00	9.33	1238	2329
8-12	20.00	4.17	9.57	10.97	1341	2523
8-17	27.00	3.56	8.00	9.41	1247	2345
9-1	1.20	3.30	7.65	8.79	1216	2281
9-3	4.43	3.53	8.02	9.28	1243	2339
9-4	5.93	2.83	6.37	7.39	1122	2110
9-5.1	7.25	2.55	5.52	6.59	1064	1996
9-5.2	7.35	2.55	5.50	6.59	1064	1996
9-8	11.75	3.16	7.12	8.34	1178	2220
9-13	20.80	2.93	6.58	7.67	1138	2141
10-1	1.10	3.26	7.32	8.56	1193	2245
10-3	4.33	3.07	7.01	8.11	1171	2196
10-4	5.83	3.49	7.92	9.17	1236	2323
10-7	9.33	4.03	9.32	10.67	1322	2487
10-9	12.25	4.17	9.57	10.50	1341	2523
10-10	13.73	3.40	7.87	9.11	1226	2303
10-18	25.42	3.79	8.71	9.97	1287	2423

Table (4). Elastic modulii ranges of Sharm El-Sheikh bottom sediments.

B.N.	(μ) N/m^2 x 10^9		(K) N/m^2 x 10^9		(E) N/m^2 x 10^9		(V_s) m/sec		(V_p) m/sec	
	Min	Max	Min	Max	Min	Max.	Min	Max.	Min	Max.
1	2.6	6.63	5.95	15.26	6.85	17.3	1086	1628	2038	3099
2	2.6	5.16	1.88	9.57	9.57	6.69	1072	1473	2011	2771
3	2.43	4.17	5.27	9.57	5.27	11.14	1047	1341	1972	2523
4	2.48	4.03	5.3	9.28	6.4	11.0	1052	1322	1985	2487
8	3.3	4.17	7.65	9.57	8.87	10.97	1216	1341	2281	2523
9	2.55	3.53	5.5	8.02	6.59	9.3	1064	1243	1996	2339
10	3.10	4.2	7.00	9.6	8.1	10.7	1171	1341	2196	2523

(e) to the shallower (in the northeastern part). Accordingly, it is recommended to follow the general direction of the Aqaba trend to be the elongation of buildings under construction. Such buildings will resist any tremor or vibration arises from an earthquake, where the stress per unit length might be minimal. This statement is probably in contradiction to another views that, the direction of energy is going from north and northeast and probably from the east towards Sharm El-Sheikh. Actually, this conclusion comes up from the analysis of a number of earthquakes, which took place along the active transform faults.

ACKNOWLEDGMENT

The authors wish to express their gratitude to Prof. M.B. Awad for the fruitful discussion, guidance and revision of the present work. Also kindly acknowledgement is offered to Prof. El-Abd for his revision the mathematical modeling. Special thanks are offered to Mr. Osama Farha for providing the material used in this work, as well as, all necessary data to accomplish this work.

REFERENCES

Abd El- Fattah, A.K. & Hussein. H. M. & Ibrahim, E. M. and Abu EATA, A.S., 1997. Fault plane solution of 1993 & 1995 Gulf of Aqaba earthquakes and their tectonic implications, Ann, digeosis.23, 381-390.

Archie, G. E., 1942. "The electrical Resistivity in determining some reservoir characteristics": American Institute of Mining & Metallurgical Engineers, Tech Pub.1422.

Archie, G. E., 1950. "Introduction to petrophysics of reservoir rocks". Bull Am Assoc. pet. Geologist, 34, pp. 943-961.

Awad, M.B. & Shata, M.A. and Farha, O.A., 1998. Paleoenvironmental conditions and sealevel changes in Sharm El-Sheikh (Gulf of Aqaba, Egypt) based on Sedimentological and mineralogical studies. Bull. Nat. Inst. Oceanog.& Fish., A.R.E,1998; vol.(24): 1-33.

Barker, R. D. & Worthington, P. F., 1973. "Some hydrographical properties of the Bunter Sandstone of North West England". Geoexploration V.II PP 151-170.

Box, G. E. P. and Jenkins, G. M., 1976. "Time Series Analysis forecasting and control", Second edition. San Francisco: Holden - Day.

Cox, D. R. and Lewis, P. A. W., 1966. "The statistical Analysis of Series of events". London: Mcthuen.

Draper, N. R. and Smith, H., 1966. "Applied Regression Analysis". New York: Wiley

El-Abd, Y., 1985. "Some Hydrogeophysical properties of coral reef sediments, near Sharm Obhur, Red Sea". Journal of Faculty of Marine Science, King Abdulaziz Univ. Jeddah, Saudi Arabia. V4, 1405H; 79- 96.

ıot, S. E. and Wiley, B. F., 1975. "Compressional velocities of partially Saturated unconsolidated sands", Geophysics, 40; 949- 954.

ınd, R.; Zak, I.; Goldberg, M.; Weisbrod, T. and Derin, B.; 1970. "The shear along the Dead Sea Rift" Philos. Trans. Roy. Soc. London, A 267-p. 107-130.

egory, A. R., 1976. "Fluid Saturation effects on dynamic elastic properties of sedimentary rocks", Geophysics, 41; 485- 921.

ahim, H. A., 1993. "Geophysical studies on offshore basins in the Gulf of Suez, Egypt", M. Sc. Thesis submitted to the Faculty of Science Cairo University.

son, P. D.; Taylor Smith, D. and Stanford, P. N.; 1975. "Resistivity-Porosity-Particle Shape relationships for marine sands", Geophysics, 43: 1250-1268.

Kenzie, D. P.; D. Davies & P. Molnar; 1970. "Plate tectonics of the Red Sea and East Africa". Nature 226: 243- 248.

rrison, D. F., 1967. "Multivariate Statistical Methods". New York: Mc Grow-Hill.

O.F., 1993. Report on "Development of sharm El- Sheikh Harbor, south Sinai Governorate", Egypt.

arazangi, M., 1983. Summary of the seismotectonism of Arab region (internal report of geological Survey of Egypt).

lhemus, N. W., 1982. "STATGRAPHICS: An interactive Statistical graphics system in Apl", proceedings of the 1982 National Computer Graphics Association conference. Anaheim, cal.

than, R.H. and Staffa, P. L., 1976. Vp/Vs- A potential Hydrocarbon Indicator, Geophysics; 41, 837- 849.

tsuoka, M.M., 1971. Multivariate Analysis. New York: Wiley.

Taylor Smith, D., 1975. Geophysical assessment of sea- floor sediments properties, Oceanology International 75 conference Papers,Brighton, 320-328.

Tukey, J. W., 1977. Exploratory Data Analysis. Reading, Mass Addison - Wesly.

Winkler, K.W. and Nur, A., 1982. Seismic attenuation effects of pore fluids and frictional sliding; Geophysics, 47,1- 15.